Computer simulation of beam steering by crystal channeling

Valery Biryukov*
Institute for High Energy Physics, Protvino, 142284 Moscow Region, Russia
(Received 2 September 1994)

The Monte Carlo computer program CATCH for the simulation of planar channeling in bent crystals is presented. The program tracks a charged particle through the deformed crystal lattice with the use of the continuous-potential approximation and by taking into account the processes of both single and multiple scattering on electrons and nuclei. The output consists of the exit angular distributions, the energy loss spectra, and the spectra of any close-encounter process of interest. The program predictions for the feed-out and feed-in rates, energy loss spectra, and beam bending efficiency are compared with the recent experimental data.

PACS number(s): 07.77.−n, 61.80.Mk

I. INTRODUCTION

Channeling of a beam of charged particles in a bent monocrystal is going to become a working tool for the next generation of accelerators [1,2]. Therefore there is a need for a theoretical tool that is able to describe a whole set of experimental data on channeling in the GeV range and also simulate the processes important for the future applications. The output should be the distribution of exiting primary and secondary particles, the energy loss in crystal, and any other interesting quantity related to channeling. Since these processes are sensitive to orientation, the simulation should track every particle through the crystal lattice, computing the probability of any process as a function of the coordinates.

Historically, one of the independent discoveries of channeling, in the early 1960s, was done in a Monte Carlo simulation of low-energy ($\leq$MeV) ions propagating in crystals [3]. The very low ranges and the thin crystals used allowed the study of binary collisions of the incident ion with the atoms of the crystal (see Refs. [4,5] and references therein). At GeV energy, crystals of a few centimetres in length are used, so tracking with binary collisions would take a considerable amount of time. Instead, an approach with the continuous potential introduced by Lindhard [6] can be used. In this approach one considers collisions of the incoming particle with the atomic strings or planes instead of separate atoms, if the particle is sufficiently aligned with respect to the crystallographic axis or plane. The validity of doing this improves with the increase of the particle energy [6].

In addition to the motion in the potential one must take into account the scattering. This makes it necessary to use either kinetic equations [7] or computer simulation [8] to transport particles through a crystal. The general feature of the methods described in Refs. [7,8] is the use of the diffusion approach, which omits the single scattering acts. However, in Monte Carlo methods it is easy to include the single collisions with nuclei and electrons. We shall see below that single electronic collisions influence the high energy channeling essentially. Such collisions with electrons shape the interesting energy loss spectra in aligned crystals, which are an essential part of the experimental technique in handling the channeled beams. Moreover, these close-encounter processes are the source of the secondary particles emitted from the crystal, thus being responsible for the background. Here we describe the Monte Carlo computer program CATCH (capture and transport of charged particles in a crystal) for the simulation of planar channeling in curved crystals, which does not use the diffusion approximation.

II. SIMULATION PROCEDURE

A. Continuous potential

For the potential of the atomic plane we use the Molière approximation with the screening length $a_{TF} = 0.8853 a_B Z^{-1/3}$, where a_B=0.529 Å, Z is the crystal atomic number (for silicon, Z=14, we have a_{TF}=0.194 Å); details can be found, e.g., in the review by Gemmel [9]. The interplanar potential is the sum of the contributions from many single planes arranged periodically. Formally, we take into account an infinite number of planes since this is easy to do analytically in the case of the Molière potential (a sum of exponents). Really, only two pairs of the nearest planes may contribute sizably. Any particle moving in crystal may traverse any atomic plane; this may matter in the case of Si(111) geometry and the like, where two different (wide and narrow) adjacent channels are present. The static-lattice potential is modified to take into account the thermal vibrations of the lattice atoms; this is done by integration over the Gaussian distribution of the atom displacement. Bending of the crystal has no effect on this potential. However, it causes a centrifugal force in the noninertial frame related to the atomic planes. To solve the equation of motion in the potential $U(x)$ of the bent crystal, as a first approx-

*Electronic address: biryukov@mx.ihep.su

imation to the transport of a particle

$$pv\frac{d^2x}{dz^2} = -\frac{dU(x)}{dx} - \frac{pv}{R(z)} \tag{1}$$

[x being the transversal coordinate, z the longitudinal coordinate, pv the particle longitudinal momentum and velocity product, and $R(z)$ the local radius of curvature] we use the fast form of the Verlet algorithm [10]

$$x_{i+1} - x_i = (\theta_i + 0.5 f_i \delta z)\delta z\,, \tag{2}$$

$$\theta_{i+1} - \theta_i = 0.5(f_{i+1} + f_i)\delta\, z, \tag{3}$$

with θ for dx/dz, f for the force, and δz for the step. It was chosen over the other second-order algorithms for nonlinear equations of motion, such as Euler-Cromer's and Beeman's, because of the better conservation of the transverse energy shown in the potential motion. For the trapped particle Eqs. (2) and (3) describe its oscillatory motion in the channel formed with atomic planes; then the angle θ is confined in the range of $\pm\theta_c$, where the critical angle θ_c is defined by the potential well depth U_0.

B. Scattering

Beam steering by a crystal is due to the trapping of some particles in the potential well $U(x)$, where they then follow the direction of the atomic planes. This simple picture is disturbed by scattering processes, which could cause (as result of one or many scattering events) the trapped particle to come to a free state (feed-out, or the dechanneling process) and an initially free particle to be trapped in the channeled state (feed-in, or volume capture).

1. Scattering on electrons

Feed-out is mostly due to scattering on electrons [7], because the channeled particles move far from the nuclei. The mean energy loss in this scattering can be written as [11]

$$-\frac{dE}{dz} = \frac{D}{2\beta^2}\left[\ln\frac{2m_e c^2\beta^2\gamma^2}{I} - \beta^2 - \delta + \rho_e(x)\left(\ln\frac{T_{\max}}{I} - \beta^2\right)\right], \tag{4}$$

with $D = 4\pi N_A r_e^2 m_e c^2 z^2 \frac{Z}{A}\rho$, z for the charge of the incident particle (in units of e), ρ for the crystal density, Z and A for atomic number and weight, and the other notation being standard [12]. The ionization potential $I \approx 170$ eV in silicon and the maximal energy transfer to a single electron is equal to

$$T_{\max} = \frac{2m_e c^2\beta^2\gamma^2}{1 + 2\gamma m_e/M + (m_e/M)^2} \approx 2m_e c^2\beta^2\gamma^2\,. \tag{5}$$

The last term in large square brackets in Eq. (4) is due to single collisions and depends on the local density $\rho_e(x)$ (normalized on the amorphous one) of electrons. The $\rho_e(x)$ value is computed from the potential $U(x)$ via Poisson equation (subtracting the nuclear density, which is discussed below). The energy T transferred in such a single collision is generated according to the distribution function

$$\frac{d^2N}{dTdz} = \frac{D\rho_e(x)}{2\beta^2}\frac{1}{T^2}\,. \tag{6}$$

The $1/T^2$ distribution is quite easy to generate by a computer. The overall probability of collision with $I \le T \le T_{\max}$ per unit length can be obtained by integration of the above equation over T. It should be mentioned that deviations from the above formula at $T \approx I$ or $T \approx T_{\max}$ are of no concern at all due to the nature of dechanneling discussed below. The momentum q transferred in a collision is equal to $\sqrt{2m_eT + (T/c)^2}$. The transverse component of q produces a (round) angular kick of

$$\theta_s = \frac{\sqrt{2m_eT(1 - T/T_{\max})}}{p}\,. \tag{7}$$

Its projections are used to modify the angles θ_x and θ_y of the particle. The energy is returned modified according to the energy loss in the crystal. In the simulation we make no distinction between the scatterings with small or large T, treating them as small or large kicks. The frequent small kicks produce, in fact, a diffusionlike angular scattering, with the mean square value given by

$$\theta^2_{\rm rms} = \frac{2m_e}{p^2}\left\langle\sum_i T_i(1 - T_i/T_{\max})\right\rangle\,. \tag{8}$$

The rare hard kicks may knock the particle out of the channeling mode at once. The distribution of Eq. (6) is continuous and there is no sharp distinction between "soft" and "hard" kicks, both in nature and in our algorithm. It must be mentioned that the problem of a "catastrophic" dechanneling, owing to a single collision of heavy particle with electron, arises only in a high energy range, starting with ~1 GeV. In the MeV range the maximal momentum transfer in such a collision is lower than one required for this "knockout." We discuss this in some detail in Sec. III.

2. Scattering on nuclei

The scattering on nuclei is divided in two parts. The soft frequent collisions are taken into account continuously at every step; the random deflection angle is computed as a Gaussian function with the root-mean-square value given by the Kitagawa–Ohtsuki approximation [13]

$$\langle\theta^2_{\rm nucl\,sc}\rangle = \langle\theta^2_{\rm sc}\rangle_{\rm am}\rho_n(x)\,, \tag{9}$$

i.e., the mean angle of scattering squared is proportional

to the local density of nuclei $\rho_n(x)$ (normalized on the amorphous value); $\langle\theta_{sc}^2\rangle_{am}$ is the scattering angle square in the amorphous substance. The density function $\rho_n(x)$ is Gaussian, with the rms value u being the thermal vibration amplitude of the atom.

The hard nuclear collisions are treated event by event. Their probability, proportional to $\rho_n(x)$, is checked at every step. If such a collision succeeds, the routine responsible for the event generation may be called. To simulate the single nuclear collisions one may use any specialized code, such as the LUND [14] routines; the CATCH program serves as a frame to provide the orientational dependence of these processes. This scheme may be used for the description of any close-encounter process of interest; then one should define the collision length properly. The secondary particles (possibly produced in interactions of the particle in crystal) may also, in principle, be tracked through the crystal lattice.

C. Crystal imperfection

The crystal curvature, both longitudinal and transverse, and the crystal plane orientation can be arbitrary functions of spatial coordinates. Any data measured (or assumed) for the real crystal shape can be implemented in the simulation. The imperfection of the crystal lattice, in the presence of dislocations, may be taken into account through the $R(z)$ term in Eq. (1).

In the case of the beam extraction from the accelerator, extremely small impact parameters are possible, making the surface effects essential. The particle entering the real crystal very close to its edge can suffer from various additional factors: a miscut angle (between the atomic planes and the surface), roughness (i.e., nonflatness) of the surface, a possible amorphous layer, and a bent surface. Therefore one must pay particular attention to the near-surface tracking, where the particle is entering and leaving the crystal material (because of the roughness, holes, and bend), both coherent and noncoherent scattering in this peculiar region, bending in short channels, and so on. The surface effects mentioned above are simulated in CATCH. The roughness is expressed by a periodical function $a\sin(2\pi z/l)$, where a is the amplitude of the "bumps" and l is their periodicity. The "rough" crystalline material can be superimposed by a uniform amorphous layer. The position of the surfaces is computed at every step in accordance with bending with the variable curvature. Every particle (both channeled and nonchanneled) is tracked in the crystal and can leak out through any surface. Near the rough surface it is even possible to leak out and be caught again many times, i.e., the particle traverses sequentially the crystal bumps and vacuum (or amorphous skin) between. The description of the program usage may be found in Ref. [15].

III. COMMENTS ON DIFFUSION APPROACH

Here we discuss a difficulty of the diffusion approach specific to the high (>GeV) energy range. The diffusion approximation for electronic scattering is employed by many authors, even in computer simulations [8,16]. In this approach one assumes that scattering on electrons is diffusionlike, i.e., the angular kick $\theta_s \ll \theta_c$ in any single collision. Then the angle of the the particle is changed by frequent infinitesimal steps, with the rms value θ_{rms} of the scattering angle given by Eq. (8). It is worth mentioning that the θ_{rms} value depends on the total amount of energy transferred, not on the detail of the distribution of Eq. (6).

In the MeV energy range (where the majority of both experimental and theoretical efforts for crystal channeling have been made), this approximation for heavy ions works perfectly well because even the maximal possible angular kick per collision $\theta_s^{max} = \sqrt{m_e T_{max}}/p \approx 1.4 m_e/M$ (M is the particle mass) is always smaller than θ_c. For example, for protons $\theta_s^{max} \approx 0.77$ mrad, while $\theta_c > 1$ mrad in silicon for a proton energy up to 10 MeV.

In the energy range of ~100 GeV (the range of modern applications of bent crystals), the θ_c value is drastically reduced down to ~10 μrad. Therefore rare catastrophic collisions with $\theta_s > \theta_c$ may happen. More generally, the weight of the hard collisions with θ_s comparable to θ_c is strongly increased. The problem for the diffusion approach is that the integration up to T_{max} in the diffusion coefficient of the Eq. (8) kind is no longer justified. The *energy* transferred with catastrophic collisions ($\theta_s > \theta_c$) is of no importance for dechanneling and therefore it should not be included into the diffusion coefficient.

Although θ_{rms}^2 depends on T_{max} via $\ln(T_{max}/I)$, we shall see below that removal of the energy transfers of catastrophic collisions from Eq. (8) reduces the diffusion coefficient by a factor of 2–3.

Nevertheless, some authors [17,8,18] use for T_{max} the maximal possible value, given by Eq. (5). The others [19,20,16] try a "cutoff," defining T_{max} as the energy transfer T_c causing the angular kick of the order of θ_c (or even much smaller [20]), because at higher T the diffusion approach is certainly invalid.

We will explain the weak points of both choices with a numerical example. For a 100 GeV proton the maximal transfer T_{max}=10 GeV. However, the transfer T_c causing the angular kick (projection) to be equal to θ_c is quite moderate:

$$T_c \approx \frac{p^2\theta_c^2}{m_e} = \frac{2M\gamma}{m_e}U_0 . \tag{10}$$

In silicon T_c= 4 MeV for a 100 GeV proton. We find that from the energy transferred via single collisions, about one-half of it is carried away in the scatterings with $\theta_s > \theta_c$. Taking these scatterings into account in Eq. (8) is inconsistent with the diffusion approximation. The problem is even deeper because for collisions with $T > T_c$, the T value is no longer important. The scatterings with T= 10 MeV and T= 1 GeV are equally essential since they knock the particle out of the channeling mode immediately. It is the probability of knockout that is important, not the energy transferred with it. Therefore, including into Eq. (8) the *energy* transferred in scatterings with $T > T_c$ (i.e., T_{max}= 10 GeV in our example)

increases the inconsistency further.

In order to take into account the above argumentation, some authors [19,20,16] cut off large transfers: $T_{\max}^{\text{cut}} \leq T_c$. One problem then is the arbitrariness of the cutoff parameter $T_{\max}^{\text{cut}}$. For example, the use of Eq. (10) instead of Eq. (5) for $T_{\max}$ decreases the diffusion coefficient by a factor of 2. In order to fit the experimental data, the allowed angle of scattering is sometimes restricted further, e.g., down to $\theta_c/20$ [20], thus reducing that coefficient even more. Such a freedom in the selection of $T_{\max}$ reduces the usefulness of the diffusion theory in the GeV energy range. Neglect of the rarer hard scattering events is another difficulty, since their contribution is lost. This may be particularly essential, e.g., for the rare process of feeding-in in the bent crystals. Another example may be the energy loss spectrum in aligned crystals. The rarer hard scatterings form the spectrum tail; on the other hand, such events influence the channeled particle state. In a diffusion-based description this link is lost. The properties (such as feed-out rates) of the channeled particles are often measured using the energy loss tagging technique (see Sec. IV); therefore an adequate theoretical approach is indispensable. Finally, in the crystal-assisted beam extraction the energy loss fluctuations may be important for the particle multiturn dynamics in the accelerator ring.

Nevertheless, the diffusion model often provides a good description of dechanneling in bent crystals. The reason may be understood if we will look at the influence of hard collisions on dechanneling. From Eqs. (6) and (10) the characteristic length, along which such a "single" feed-out occurs, may be estimated as

$$L_{\text{single}} = \frac{2\beta^2 T_c}{D\langle\rho_e(x)\rangle} = \frac{4pvU_0}{Dm_e c^2\langle\rho_e(x)\rangle} . \tag{11}$$

It has much the same functional dependence (except for a logarithmic factor) on the properties of crystal and incident particle as the dechanneling length in the diffusion model, i.e., $L_D \sim pvU_0/z^2$ [7]. This similarity remains in a bent crystal: $L_D, L_{\text{single}} \sim U_0(pv/R)$. Therefore, in a regular case the diffusion approach may fit the experimental data reasonably well. With use of the Lindhard potential Eq. (11) may be transformed further:

$$L_{\text{single}} = \frac{4a_{TF}d_p pv}{ze^2} \quad ; \tag{12}$$

the detail of the transformation from (11) to (12) can be found in Ref. [21].

IV. SIMULATION OF EXPERIMENTS

In the past few years a number of important crystal channeling experiments have been performed in the energy range of ~100 GeV. These studies provided essential data on the feed-out and feed-in rates in bent crystals, precise measurement of efficiency of the beam bending or extraction from accelerators, the energy loss spectra in aligned crystals, etc. Below we test the CATCH predictions versus some recent experimental data.

A. Energy loss

When a beam is aligned with respect to the atomic planes, the particle distribution over the transverse coordinate x undergoes an essential change, resulting in the beam splitting into the "channeled" and "random" fractions [6] (see Fig. 1). This change affects, via Eq. (4), the energy loss spectrum. This spectrum therefore is also remarkably splitted into the channeled and random (or quasichanneled) fractions, thus providing an easy way to distinguish between these two sorts of particle motion (see [22] and references therein). The energy loss spectra in the aligned crystals have been studied in experiments extensively.

Here we show only one example of a simulation, performed under the same conditions as the experiment Jensen *et al.* [23]. The proton beam of 450 GeV/c momentum passed through the aligned crystal of Si(111). The divergence of the incident beam, 35 μrad full width at half maximum, was comparable to the critical angle $\theta_c \approx 9$ μrad. In the simulation we take the flat incident angular distribution with the full width of 35 μrad. The energy lost by protons in the forthcoming, 3 mm long, part of the crystal during simulation is shown in the spectra of Fig. 2. Figure 2(a) is for the ΔE spectrum in the disaligned crystal, showing the well-known Landau distribution. Figure 2(b) is for the perfectly aligned crystal. Here, about 15% of all particles are in the peak of lower losses; this is in agreement with the ~20% observed in the experiment. Such a reduction in the energy loss is due to lower mean local electron density experienced by channeled protons. The right peak in Fig. 2(b) is shifted to the larger energy loss, when compared to the case of a disaligned crystal. This known effect is the result of the higher mean electron density (than in an amorphous substance) experienced by quasichanneled protons.

Very recently the energy loss for channeled protons has been studied thoroughly in the experiment [24] by making use of bent crystals. This experiment has been sim-

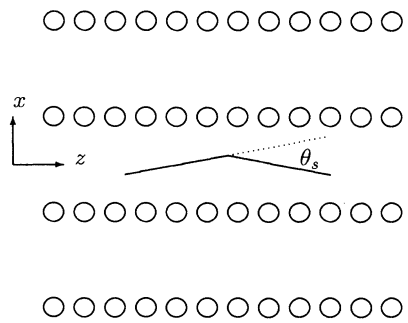

FIG. 1. Geometry used in the simulation. The particle moves on the (x, z) plane in the z direction. The atomic layers and the scattering event are shown.

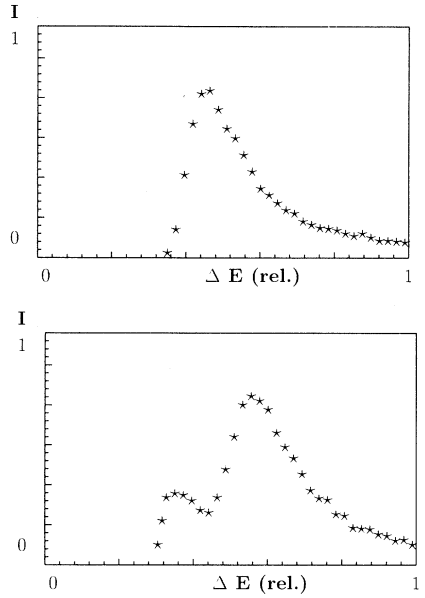

FIG. 2. Spectra of energy loss for the 450 GeV/c protons in Si(111) crystal. Simulation of the experiment [23] (a) for the disaligned crystal and (b) the perfectly aligned crystal.

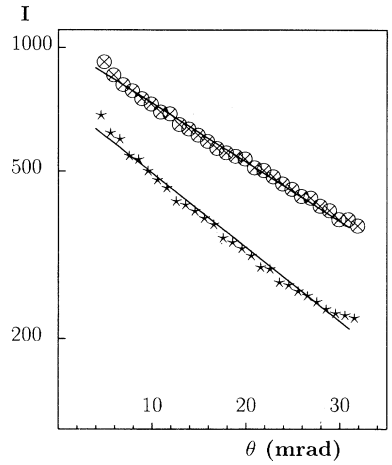

FIG. 3. Number of 150 GeV/c channeled protons as a function of the bend angle, from the simulation of the experiment [25]. The top curve is for the cooled crystal (128 K) and the bottom curve is for 293 K. The exponential fit is shown.

ulated, with the results being in good agreement with measurement. We hope to report these results in some detail elsewhere.

B. Feeding out

The comprehensive study of dechanneling has been performed by Forster *et al.* [25], where the proton feed-out rate in the Si(110) crystal, bent with a radius ≈80 cm, was measured as a function of the beam momentum in the range of 60–200 GeV/c, at two different temperatures of the crystal, 293 K and 128 K. The experimental procedure included the selection of the particles with lower energy loss in the straight part of the crystal (by means of a diode implanted). The exit angular distribution of the selected particles was integrated, from a variable θ to the full bend angle, and then fitted with an exponential function. Because of the crystal bending with uniform curvature, this angular distribution may be easily converted into the exponential-like dependence of the beam channeled fraction as a function of z, $\sim \exp(-z/L_D)$. The characteristic length L_D is called the *dechanneling length.*

The selection procedure may essentially influence the ensemble of particles used for the dechanneling measurements. Therefore it is important to take into account the selection technique in the theoretical consideration. Such a consideration, aiming to verify the widely used experimental technique, has been performed here. In the simulation we followed exactly the experimental procedure. The incoming beam had a divergence larger than θ_c. The crystal had a straight initial part and the protons showing a lower energy loss in it were selected [from a spectrum like that of Fig. 2(b)]. The examples of the integrated exit angular distribution, together with exponential fits, are shown in Fig. 3. The dechanneling lengths obtained in such a procedure are plotted in Fig. 4, together with the experimental ones. The simulation gives a reasonable approximation, overestimating L_D by ~10%. The rise of the temperature effect for L_D at the crystal strong bend is also confirmed by simulation. For an interpretation of these dependences in the diffusion model see, e.g., Ref. [26]. The simulation of this experiment, in a diffusion approach and without selection by the energy loss, was reported earlier in Ref. [8].

The bending dechanneling factors were determined in the same experiment by measuring the ratio N_1/N, N being the number of particles selected by low energy loss and N_1 those of N that exit the crystal undeflected. The same procedure repeated in our simulation gave the N_1/N values plotted in Fig. 5. The dechanneling is again

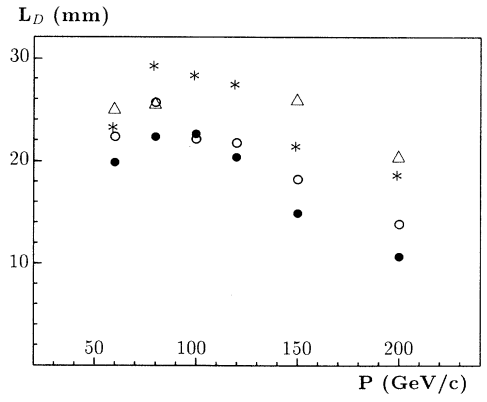

FIG. 4. L_D values from the experiment [25] (• and ∗) and the simulation (o and △). The • and o dots are for 293 K, the ∗ and △ dots are for 128 K.

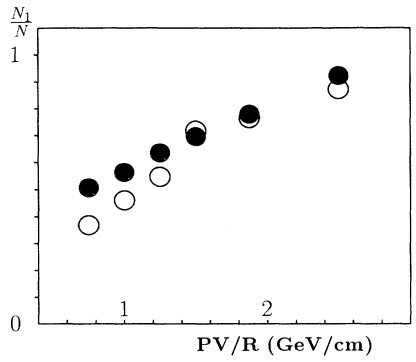

FIG. 5. Ratio N_1/N (N being the number of particles selected by low energy loss and N_1 those N which exit the crystal undeflected) as function of beam momentum. Solid dots are for the experiment [25] and open dots are for the present simulation.

underestimated on average by ~10%, with a deviation seen for smaller momenta. This may be due to the energy loss selection criterion being different from that used in the experiment of Ref. [25].

C. Feeding in

The most detailed study of the feed-in in the bent crystals has been performed in the experiments with a 70 GeV proton beam, reported in Refs. [27,21]. In Ref. [21], in addition, the crystal transmission of the trapped (fed-in) protons was investigated. The dechanneling length for this sort of particles was measured for silicon crystals with (110) and (111) orientations. This measurement used a method different from that of Ref. [25], without selection by energy losses.

For this energy range and typical crystal, the feed-in probability is quite low, $\sim 10^{-3}$. The distribution of the trapped particles is unusual, being peaked at the potential well top. This is a challenge for the simulation, making the comparison to the experiment very interesting. In the simulation we have traced by CATCH up to a half million protons in bent crystals Si(110) and Si(111), matching the experiment [21]. The dechanneling in both the experiment and the simulation was exponential-like in the angular range studied. For the bending radius of 3 m and the energy of 70 GeV, the following dechanneling lengths have been observed:

$$L_{\rm expt}^{(110)} = (37 \pm 5)\ \text{mm},\ L_{\rm expt}^{(111)} = (52 \pm 2)\ \text{mm},$$

$$L_{\rm sim}^{(110)} = (39 \pm 3)\ \text{mm},\ L_{\rm sim}^{(111)} = (40 \pm 4)\ \text{mm}.$$

The simulation results are close to the experimental ones, although the difference between the (111) and (110) planes is not seen beyond the statistical errors.

The feed-in probability values, being defined for the particles captured in "stable states," which dechannel with exponential law, are summarized in Table I. The values predicted by a simple phenomenological model [28] (namely, $R\theta_c/L_D$, where θ_c is the Lindhard angle) are given also. More details on both the simulation and the experiment may be found in Ref. [21]. Unlike the qualitative analysis of Ref. [8], here we have made clear quantitative predictions for the feed-in rate, which are in good agreement with the experimental data obtained so far.

TABLE I. The probability (in %) of the feed-in into "stable states" for a 70 GeV proton in Si crystal bent with R=3 m, from the experiment [27], the present simulation, and the model [28].

Crystal	Model	Simulation	Experiment
111	0.13	0.17±0.02	0.23
110	0.18	0.23±0.02	

The second mechanism of feeding in, namely, a reverse to the bending dechanneling, is also known theoretically, with the efficiency given roughly by $R'\lambda/2R$ ($R' = dR/dz$ is the curvature radius gradient and λ is the oscillation period of channeled particle) [29]. Unfortunately, except for the evidence of Ref. [27], the experimental check is missing.

D. Bending efficiency

Bent crystal transmission depends on the factors discussed above. In applications so far the efficiency was limited by a low ratio of critical angle θ_c to the beam typical divergence. This limitation was overcome in the series of experiments with a highly parallel "microbeam" of 450 GeV/c protons [30,23,24,31]. These studies have made a breakthrough, bringing the beam bending efficiency to values of 10% in the first experiment [30], and then up to ~50% in the very recent work [24].

Here we report simulation results for the RD22 experiment with the same microbeam on the H8 beam line. More details on both the experiment and the simulation may be found in Ref. [31]. The beam of 450 GeV/c protons was bent by a silicon (110) crystal 3 cm long. Both the crystal and the bending device were a copy of the ones used in a SPS extraction experiment. The bending angles of 8.5, 5.7, and 3.0 mrad have been used. The rms angular spread of the incoming particles was measured to be 16±2 μrad. The efficiencies found in both the experiment and the simulation are listed in Table II. The last two columns of the table show the efficiencies found for the particles incident in the $\pm\theta_c$ ($\approx \pm 7$ μrad) angular range. The simulation of the SPS experiments on crystal extraction with CATCH has been reported elsewhere [32].

V. CONCLUSIONS

The fair agreement found between the high energy crystal channeling experiments and the modern simula-

TABLE II. Efficiency of the 450 GeV/c proton beam deflection with Si(110) crystal, obtained in the experiment and the simulation [31]. The bottom numbers show the efficiency for protons incident in the $\pm\theta_c$ range. The errors given are statistical only.

Bending angle (mrad)	Efficiency (%) Experiment	Efficiency (%) Simulation (rms,15 μrad)	Efficiency (%) in the $\pm\theta_c$ Experiment	Efficiency (%) in the $\pm\theta_c$ Simulation
3.0	20±2	20.9±0.8	54±2	56±4
5.7	10±1	15.2±0.5	33±5	39±2
8.5	7.7±0.3	8.8±0.5	16±3	26±2

tion methods provides a good understanding of the feed-in and feed-out mechanisms for a high energy beam channeled in a bent perfect crystal. The confidence achieved allows us to make reliable predictions for a broad range of present and future applications, thus making the bent crystals a routine instrument for the optics of particle beams. Further work is likely needed in two directions: a full understanding of crystal extraction mode at an accelerator, and a better understanding of the crystal lattice imperfection influence on high energy channeling.

ACKNOWLEDGMENTS

The hospitality of the Pisa INFN and the CERN SL Division, where part of this work has been done, is gratefully acknowledged.

[1] B.N. Jensen *et al.*, CERN Reprot No. DRDC/P29, 1991 (unpublished).
[2] R.A. Carrigan, Jr. *et al.*, Fermilab Report No. P853, 1991(unpublished).
[3] M.T. Robinson and O.S. Oen, Phys. Rev. **132**, 2385 (1963).
[4] M.T. Robinson, Phys. Rev. B **4**, 1461 (1971).
[5] J.H. Barrett, Nucl. Instrum. Methods B **44**, 367 (1990).
[6] J. Lindhard, Kgl. Danske Vid. Selsk. Mat. Fys. Medd. **34**, 14 (1964).
[7] Y.-H.Ohtsuki, *Charged Beam Interaction with Solids* (Taylor & Francis, London, 1983).
[8] A.M. Taratin and S.A. Vorobiev, Nucl. Instrum. Methods B **47**, 247 (1990).
[9] D.S. Gemmel, Rev. Mod. Phys. **46**, 129 (1974).
[10] H. Gould and J. Tobochnik, *Computer Simulation in Physics* (Addison-Wesley, Reading, MA, 1988), Pt. I.
[11] H. Esbensen and J.A. Golovchenko, Nucl. Phys. A **298**, 382 (1978); H. Esbensen *et al.*, Phys. Rev. B **18**, 1039 (1978).
[12] Particle Data Group, Phys. Lett. B **239**, (1990).
[13] M. Kitagawa and Y.H. Ohtsuki, Phys. Rev. B **8**, 3117 (1973).
[14] The LUND Monte Carlo Programs, CERN, 1989.
[15] V.M. Biryukov, CATCH 1.4 User's Guide; CERN Report No. 93-74, 1993 (unpublished).
[16] A.M. Taratin and S.A. Vorobiev, Zh. Tekh. Fiz. **55**, 1598 (1985).
[17] Y.H. Ohtsuki and H. Nitta, in *Relativistic Channeling*, edited by R.A. Carrigan, Jr. and J. Ellison (Plenum, New York, 1987), p. 59.
[18] N.A. Kudryashov, S.V. Petrovskii, and M.N. Strikhanov, Zh. Tekh. Fiz. **59**, 68 (1989).
[19] A.M. Taratin *et al.*, Phys. Status Solidi B **100**, 273 (1980).
[20] A.M. Taratin and S.A. Vorobiev, Phys. Status Solidi B **107**, 521 (1981).
[21] V.M. Biryukov *et al.*, Nucl. Instrum. Methods B **86**, 245 (1994).
[22] E. Uggerhøj, in *Relativistic Channeling* (Ref. [17]), p. 5.
[23] B.N. Jensen *et al.*, Nucl. Instrum. Methods B **71**, 155 (1992).
[24] S.P. Møller *et al.*, Nucl. Instrum. Methods B **84**, 434 (1994).
[25] J.S. Forster *et al.*, Nucl. Phys. B **318**, 301 (1989).
[26] M.D. Bavizhev *et al.*, Zh. Tekh. Fiz. **61**, 136 (1991) [Sov. Phys. Tech. Phys. **36**, 203 (1991)]; Radiat. Effects **25**, 139 (1993).
[27] Yu.A. Chesnokov *et al.*, Nucl. Instrum. Methods B **69**, 24 (1992).
[28] V.M. Biryukov *et al.*, Nucl. Instrum. Methods B **73**, 158 (1993).
[29] V.M. Biryukov, Radiat. Effects **25**, 143 (1993).
[30] S.P. Møller *et al.*, Phys. Lett. B **256**, 91 (1991).
[31] V.M. Biryukov, G. Carboni, and F. Costantini, INFN Report, 1992 (unpublished); F. Costantini, Nucl. Instrum. Methods A **333**, 125 (1993).
[32] V.M. Biryukov, CERN Report No. 93–78, 1993 (unpublished).